Indoor Localization Accuracy Estimation from Fingerprint Data

Artyom Nikitin*, Christos Laoudias†, Georgios Chatzimilioudis†, Panagiotis Karras‡, Demetrios Zeinalipour-Yazti§†

*Skoltech, 143026 Moscow, Russia
† University of Cyprus, 1678 Nicosia, Cyprus
‡Aalborg University, 9220 Aalborg, Denmark
§Max-Planck-Institut für Informatik, 66123 Saarbrücken, Germany

artem.nikitin@skolkovotech.ru; {laoudias, gchatzim, dzeina}@ucy.ac.cy; panos@cs.aau.dk; dzeinali@mpi-inf.mpg.de

***Abstract*—The demand for *indoor localization* services has led to the development of techniques that create a *Fingerprint Map (FM)* of sensor signals (e.g., magnetic, Wi-Fi, bluetooth) at designated positions in an indoor space and then use FM as a reference for subsequent localization tasks. With such an approach, it is crucial to assess the quality of the FM before deployment, in a manner disregarding data origin and at any location of interest, so as to provide deployment staff with the information on the quality of localization. Even though FM-based localization algorithms usually provide accuracy estimates during system operation (e.g., visualized as uncertainty circle or ellipse around the user location), they do not provide any information about the expected accuracy before the actual deployment of the localization service. In this paper, we develop a novel framework for quality assessment on arbitrary FMs coined *ACCES*. Our framework comprises a generic interpolation method using *Gaussian Processes* (GP), upon which a *navigability score* at any location is derived using the *Cramer-Rao Lower Bound* (CRLB). Our approach does not rely on the underlying physical model of the fingerprint data. Our extensive experimental study with magnetic FMs, comparing empirical localization accuracy against derived bounds, demonstrates that the navigability score closely matches the accuracy variations users experience.**

I. Introduction

Site survey tools (e.g., Ekahau.com, tamos.com, inssider.com) are typically used to generate radio coverage heatmaps of indoor spaces based on readings collected during the, so called, measurement campaigns. Such heatmaps visualize the signal strength around the available Wi-Fi Access Point (AP) transmitters of an indoor space using a color map. Looking at the heatmap at different granularities, one can determine where sensor readings are deteriorated by electronics, appliances, physical barriers and subsequently improve the situtation by installing additional APs or by engaging users to contribute more measurements. Even though such heatmaps are useful, they only provide limited information about the positioning accuracy one will experience using an indoor positioning system. For example, the WiFi APs that are deployed to serve users inside a large open-plan area will have relatively strong signals across this area, yet the positioning accuracy might be low, because the signals do not vary significantly to effectively distinguish different locations.

At the same time, modern positioning systems are expected to deliver not only location estimates, but also information about the accuracy of such estimates. For example, after a localization request in any popular mobile navigation app it typically also displays a 'blue disc' centered at the user's location, whose radius denotes the level of accuracy. Such information about the computed location is highly desirable and greatly improves the user experience. Nevertheless, it is only available to the user *online* (i.e., after the location request) based on the type of used localization technology (e.g., IP, Wi-Fi ID, Cellular ID or GPS localization).

From the perspective of the deployment staff though, aiming for a higher-accuracy localization service, it is important to know the positioning quality in different areas of a building in *offline* mode, i.e., shortly after the data for the measurement map is collected, prior to any location request. A system operator who is aware that low accuracy is expected in some part of a building could take action to extend the positioning infrastructure (e.g., install additional beacons) and/or offer incentives to crowdsourcers to contribute more data in that area. Likewise, a third-party application provider might choose not to offer a service (e.g., location-aware advertisements and coupons or gaming) inside a certain venue until a minimum level of positioning accuracy is guaranteed.

Hybrid localization services [1] fuse multiple data sources to obtain both outstanding accuracy and robustness in face of data shortages. To exploit such services, an indoor localization service provider should be able to integrate new data sources and types. A common approach provides such integration capability by treating sensor measurements as *fingerprints*, each associated with a location. In the offline phase, such fingerprints are collected into a *Fingerprint Map* (*FM*) and stored in a database; subsequently, in the online phase, they are compared to readings from incoming user location requests. This *FM* approach treats all data sources equally, representing each fingerprint as a set of values associated with a location. For example, our in-house *Anyplace*[1] Indoor Navigation Service [2] utilizes crowdsourcing-based fingerprint collection and achieved an average localization accuracy of 1.96 meters [3] by using Wi-Fi and IMU data.

In this paper, we devise a generic framework that provides offline positioning accuracy assessment on arbitrary *FM*s. Our framework, titled *ACCES* (comes from "ACCuracy EStimation"), achieves this by calculating a *navigability score*, disregarding data origin, at any location of interest. Our approach comprises three steps: First, we apply a black-box technique for interpolating arbitrary fingerprints based on a widely used

[1]Available at: `http://anyplace.cs.ucy.ac.cy/`

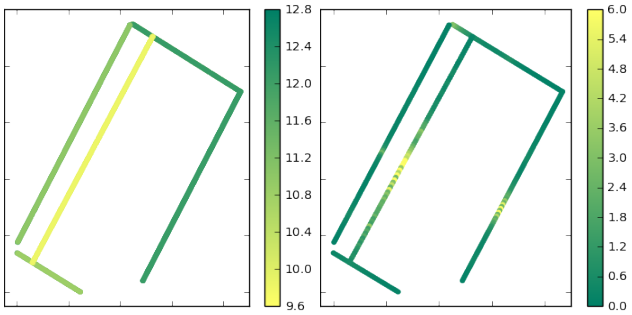

(a) Spatial fingerprint density (b) Localization error, m

Fig. 1: (a) Spatial density of collected fingerprints (count per meter) in an indoor environment. (b) Localization error (in meters) using the same data. The two plots show that there is a mismatch between fingerprint density and real localization accuracy.

statistical tool called *Gaussian Processes* (GP) [4], suitable for modeling smooth noisy data. This tool allows to: (i) predict sensor readings at chosen locations given the initial input data (*FM*); and (ii) estimate the uncertainty of such predictions in the form of the variance of a Gaussian distribution. Then, given the predictive distribution calculated with the interpolation technique, we derive a lower bound for the uncertainty in the location estimation, i.e., the *localization error*, in the form of *Cramer-Rao Lower Bound* (CRLB). The CRLB is used in estimation theory to derive lower bounds on the variance of an estimator. Obtaining such a lower bound on localization error is important for navigation service providers as it: (i) shows theoretical accuracy limitations of a service; and (ii) gives an insight on how real localization accuracy could be improved. We utilize the derived CRLB as the navigability score for *FM* at any location and apply it to real-world fingerprint data.

Visualized in a user-friendly form (e.g., as a heatmap), this navigability score can be used by an architect of a localization service to either take actions towards improving the collected *FM* by increasing the density of fingerprints, or to decide on exploiting other data sources at locations of low score. For instance, Fig. 1(a) shows the colored magnetic field heatmap over a set of indoor corridors. Even though sensor readings are very dense (i.e., most of the regions are green), and each fingerprint contains more than one value (e.g., three components of a magnetic field vector), the localization accuracy, as shown in Fig. 1(b), downgrades at certain locations of insufficient variation. As such, our propositions pave the way towards a deep understanding of where localization data fails to provide the expected localization accuracy at the pre-deployment, rather than the post-deployment stage.

This paper proposes a complete framework for indoor Accuracy Estimation coined *ACCES*. Our framework encompasses the following contributions:

- We propose a generic interpolation technique for arbitrary fingerprint maps by *Gaussian Process Regression* (GPR), allowing to predict both measurements and their uncertainty at any location of a venue.
- Given the interpolation of fingerprints and corresponding uncertainties, we derive a theoretical upper bound on localization accuracy in the form of a CRLB, which can be utilized as a navigability score.
- We demonstrate the usefulness of the proposed navigability score on real-world magnetic fingerprint data.

II. Background and Related Work

This section provides background and related work on indoor localization as well as on techniques to estimate the accuracy of localization with a fingerprint map.

A. Indoor Localization

The localization literature is very broad and diverse as it exploits several technologies[5], [2]. Satellite positioning is ubiquitously available but has an expensive energy tag, may be negatively affected by the environment (cloudy days, forests, downtown areas), and is not available indoors. The localization research community has proposed numerous alternative solutions, including Infrared, Bluetooth [6], [7], Wireless LANs [8], [9], [10], Ambient Magnetic Field [11], Artificial Quasi-static Electromagnetic Field [12], Visual and Acoustic Analysis [13], Inertial Measurement Units (IMU) [14], Ultra-Wide-Band (UWB), and Sensor Networks, and their combinations in hybrid systems [15].

In terms of data modeling, indoor localization algorithms can be categorized into: (i) *pure modeling* [16], where locations are estimated based on user-collected online measurements and a priori system information, e.g., positions of the Wi-Fi APs or Bluetooth beacons; (ii) *fingerprint-aided modeling* [17], where both user and AP locations are estimated based on user-collected online measurements and some pre-collected location measurements called *fingerprints*; and (iii) *pure fingerprinting* [8], which is based solely on the similarity of online measurements with pre-collected fingerprints.

An advantage of *pure fingerprint-based* indoor localization algorithms is their applicability regardless of the underlying data sources [11], [18], [13]. Several techniques collect sensor measurements (e.g., radio signals from Wi-Fi APs or Bluetooth beacons, magnetometer and light sensor readings), and store them in a database at high density. For instance, a smartphone's magnetometer[2] readings comprise of 3 values each, corresponding to the magnitude and direction (with respect to the measuring device's reference frame) of the earth's ambient magnetic field combined with the magnetic field from other sources, such as electronic devices. For indoor localization purposes, such fingerprints are collected at certain locations (x, y), pin-pointed on a building floor map (e.g., every few meters) in an offline phase. Subsequently, these fingerprints are joined in an $N \times 3$ matrix, the *Fingerprint Map* (*FM*), where N is the number of unique locations. Users can then compare observed magnetometer measurements against the *FM* in order to find the best match, using algorithms such as k Nearest Neighbor (kNN) algorithm or its popular Weighted kNN (WkNN) variant [19].

[2]In this paper we experimentally focus on magnetic data, but the scope of our solution also covers any other types of data such as Wi-Fi.

B. Accuracy Estimation

The goal of estimating localization accuracy is to predict the error between the computed location and the actual location of a user given noisy measurements along with fingerprint and/or system data. In this paper, we focus on estimating the achievable accuracy given only a fingerprint map, in the context of pure fingerprinting. Here, we present the literature on the accuracy estimation problem.

An approach for *online* localization confidence estimation is proposed in [20]; this technique does not require knowledge of the underlying localization algorithm. However, it can be only used online, as accuracy estimation can be given only when using a localization service. Authors in [21] propose algorithms for *offline* localization accuracy estimation based on spatial measurements' diversity. One of the proposed approaches involves splitting the indoor environment into small clusters and merging adjacent clusters based on the similarity of *Radio Signal Strength Indicator* (RSSI) distributions. A cluster's final size indicates the localization accuracy that can be achieved at its area. While practical enough, this solution lacks a formal model to allow providing strong guarantees. In this work, we address the problem of offline localization accuracy estimation, but do this in a more theoretical manner.

To obtain a strict theoretical estimate, works such as [16], [22], [23] employ the *Cramer-Rao Lower Bound* (CRLB), i.e., a lower bound on the variance of estimators. In particular, [16] uses a CRLB to estimate the localization accuracy for several motion models and wireless sensor measurements (e.g., signal strength, time of arrival), and investigate whether particular policy requirements can be met; [22] uses CRLB to estimate the accuracy achieved by the *Signal Strength Difference* (SSD) on a signal strength propagation model. Likewise, [23] uses CRLB to estimate the localization accuracy for wireless data and optimize AP placement. Nevertheless, in all the above techniques, the predicted accuracy depends on the particular measurement model, constraining their generality, and even imposing inapplicability if the model is unknown (which is the case for the ambient magnetic field data). The first work to propose fingerprint-based localization using Gaussian Process Regression was [24]; however, it does not provide estimates on the accuracy of localization with CRLB as we do in this paper, but rather on the parameters of GPR.

Swangmuang and Krishnamurthy in [25] propose an analytical model based on *proximity graphs* to determine the probability of correct localization in fingerprint-based localization systems. However, this model is not geared towards predicting or bounding the actual localization error.

III. System Model and Problem Formulation

This section formalizes our system model assumptions, upon which a problem definition is provided. The main notation we use is presented in Table I.

A. System Model

We assume an indoor area I, with the d_r-dimensional coordinates of locations in this area denoted as $\mathbf{r} \in \mathbb{R}^{d_r}$. A fingerprint map FM of some data source for this area is a set of *fingerprints*, each represented as a pair of vectors of:

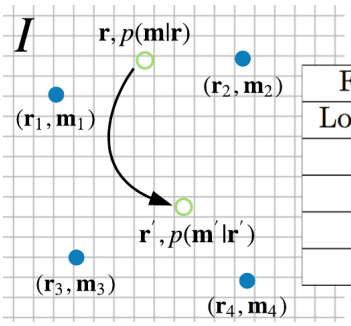

Fingerprint Map (FM)	
Location	Measurements
$\mathbf{r}_1$	$\mathbf{m}_1$
$\mathbf{r}_2$	$\mathbf{m}_2$
...	...
$\mathbf{r}_N$	$\mathbf{m}_N$

Fig. 2: System Model: (i) a user (empty circles) moving in an area with probability $p(\mathbf{m}|\mathbf{r})$ to measure $\mathbf{m}$ at $\mathbf{r}$; (ii) Fingerprint Map FM.

(i) a measurement (e.g., RSSI, magnetometer reading) and (ii) an associated position where these values were collected, i.e., $FM = \{(\mathbf{r}_i, \mathbf{m}_i) : i = 1, ..., N,\ \mathbf{r}_i \in \mathbb{R}^{d_r},\ \mathbf{m}_i \in \mathbb{R}^{d_m}\}$, where N is the size of the FM and $\mathbf{m}_i$ is the d_m-dimensional vector of measurements at location $\mathbf{r}_i$.

TABLE I: Used Notation

Notation	Description
I	Indoor space
FM, N	Fingerprint Map and its size
L, M	Set of locations of interest and its size
$\mathbf{r}$, d_r	Coordinate-vector and its dimensionality
$\mathbf{m}$, d_m	Measurement vector and its dimensionality
$\boldsymbol{\theta}$, d_θ	Estimated parameter and its dimensionality
$\mathbf{x}$, d_x	Observed random-vector and its dimensionality
$p(\mathbf{x}\|\boldsymbol{\theta})$	Likelihood of observing $\mathbf{x}$ given $\boldsymbol{\theta}$
$\mathcal{I}(\boldsymbol{\theta})$	Fisher Information Matrix
$\mathbb{E}(\cdot), \mathbb{D}(\cdot)$	Expectation and Dispersion of a random variable
$\lvert\cdot\rvert, (\cdot)^{-1}, tr(\cdot)$	Determinant, inverse and trace of a square matrix
$cov(\cdot)$	Covariance matrix of a random vector

B. Problem Formulation

We formulate the task of offline accuracy estimation for fingerprint-based localization in two steps: (i) given a fingerprint map FM, find the likelihood $p(\mathbf{m}|\mathbf{r})$ that $\mathbf{m}$ will be measured at location $\mathbf{r}$; (ii) given the likelihood $p(\mathbf{m}|\mathbf{r})$ find the smallest possible achievable *Root-Mean Square Error* (RMSE) of the position estimation at some location $\mathbf{r}$. Such a bound on the RMSE at an arbitrary location can be used as a *navigability score*, which depicts the localization quality there.

We conjecture that changes in the observed RMSE along locations would be reflected in corresponding changes in the calculated score. We assess our hypothesis as follows: (i) given the fingerprint map FM, we evaluate the navigability score and the RMSE of location estimation using the WkNN algorithm at a subset of locations $L = \{\mathbf{r}_j : j = 1, ..., M\}$; and (ii) we calculate the *relative similarity* between the respective values of RMSE and the navigability score. Since the navigability score may be defined not only as a lower-bound on RMSE, but in arbitrary manner carrying any unit measure and physical meaning, it is not possible to directly compare real localization error with it. Therefore, we construct

the relative similarity so that it captures not difference in the values, but rather difference in relative changes (over space) of the values. We assume L to comprise not 2-D but 1-D locations (i.e., $d_r = 1$) in order to simplify the calculations, and moreover, without loss of generality, we assume they are sorted by coordinate values.

Similarity Metric: Now, we describe how we calculate such relative similarity. Let $X = X_j$ and $Y = Y_j$ denote sets of values associated to the 1-D locations $r_j \in L$. Then, we define a similarity measure between these sets as follows: (i) to capture the behavior of X and Y, we calculate their *Difference Quotients* (DQ), $DQ(X_j)$ and $DQ(Y_j)$ for X and Y at each location $r_j \in L$; (ii) to evaluate the distance between the respective DQs we apply sequences similarity measure algorithm, which we choose to be *Dynamic Time Warping* (DTW); and (iii) we normalize the obtained distance value to the $[-1; 1]$ domain, where 1 corresponds to identical behavior, 0 to dissimilar, and -1 to opposite behavior.

The Difference Quotient is a discrete approximation of a function's derivative, showing how the function grows or decreases (i.e., the measure for the average rate of change); thus, it is suitable for a qualitative description of a function's behavior. In our setting it is calculated as follows:

$$DQ(X_j) = \frac{X_j - X_{j-1}}{r_j - r_{j-1}},\ j = 2, ..., M \tag{1}$$

The boundary case for X_1 can be treated differently and is not of significant importance, we let $DQ(X_1) = DQ(X_2)$, $DQ(Y_j)$ is calculated similarly.

DTW allows for the comparison of temporal sequences that may vary in speed, i.e., data values may be shifted and/or stretched relatively. DTW accommodates such deformations, as a *window size* parameter allows, and finds the dislocations that minimize a distance function. For example, consider the sequence $X_j = [0, 0.1, 0.2, 0.3, 0.4, 0.5]$ and its element-wise square $Y_j = X_j^2$; the sum of element-wise absolute differences $\sum |X_j - Y_j|$ yields 0.95, whereas DTW with window size 2 gives value of 0.72, and, with window size 6, value 0.55.

The DTW result is a pair of optimally warped DQ-sequences $DQ(X)'$ and $DQ(Y)'$, on which the optimal DTW distance function is obtained. Given these M' warped sequences, we compute the Relative DQ-Similarity $DQRelSim$ as follows:

$$\begin{aligned} &DQRelSim(X, Y) = \\ &= -\frac{1}{M'} \sum_{j=1}^{M'} \frac{|DQ(X_j)' - DQ(Y_j)'|}{\max\left(|DQ(X_j)'|, |DQ(Y_j)'|\right)} + 1. \end{aligned} \tag{2}$$

If $DQ(X_j)' = DQ(Y_j)'$, then $DQRelSim(X, Y) = 1$, and if $DQ(X_j)' = -DQ(Y_j)'$, then $DQRelSim(X, Y) = -1$. Moreover, if, say, X is constant, and, thus, $DQ(X_j)$ and $DQ(X_j)'$ are all zero, whereas Y is varying, then, from the construction of the normalization step, $DQRelSim(X, Y) = 0$. As it is shown in the experimental section, two sequences X and Y (i.e., RMSE and the navigability score values) are considered to behave similarly if $DQRelSim(X, Y) \geq 0.1$.

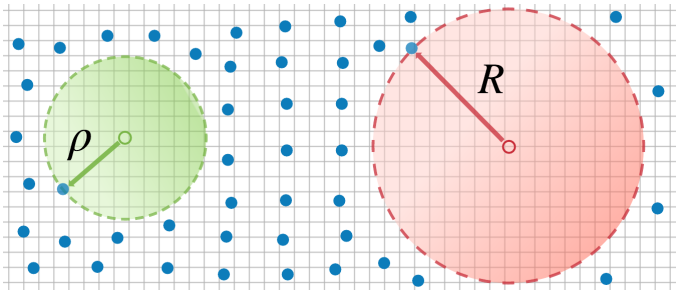

Fig. 3: *FSSI*: $FSSI_{green} = 4\pi\rho^2$, $FSSI_{red} = 4\pi R^2$. Higher FSSI values correspond to locations of lower *FM* density.

C. Naïve Approach

A basic approach for *FM* assessment could be based on the map's spatial sparsity. We can measure the spatial sparsity at a location $\mathbf{r}$ via simple navigability score called *Fingerprint Spatial Sparsity Indicator* (FSSI), defined as the area of a circle centered at $\mathbf{r}$ and touching its nearest fingerprint (see Fig. 3):

$$FSSI(\mathbf{r}) = \min_{i \in 1,...,N} \|\mathbf{r} - \mathbf{r}_i\|, \tag{3}$$

where $\mathbf{r}_i$ denotes the $i-$th fingerprint in FM. Presumably, accuracy should be lower (equivalently, RMSE should be higher) at locations with high FSSI values, as less information is obtained with fewer collected fingerprints. Yet this approach will be shown in our experimental section to be inadequate, as, even with high *FM* density, the measured values may vary a little over space, leading to accuracy degradation.

IV. The *ACCES* Framework

In this section we describe *ACCES*, which is a novel framework for offline quality assessment of arbitrary fingerprint maps. We outline its structure and then describe its internal calculation steps, namely the Fingerprint Prediction and the Accuracy Estimation.

A. Outline of the Solution

To develop a navigability score for arbitrary fingerprint maps we consider two steps:

1) **Fingerprint Prediction:** Given a set of fingerprints on an indoor map we interpolate them to any location on the map using GPR. The interpolation output comprises the predicted values and their uncertainty in the form of a Gaussian distribution's mean and variance, respectively. This step allows to construct the picture of the possible signal (e.g., Wi-Fi or magnetic) distribution over the whole indoor map along with the confidence in such distribution.
2) **Accuracy Estimation:** Given such an interpolation of the fingerprints, we derive a bound on the best possibly achievable accuracy in the form of CRLB, which we set as our ACCES navigability score. This step helps in finding the best localization accuracy that can be achieved at certain location given the confidence in the constructed signal distribution.

The first step allows us to perform FM interpolation disregarding the data source to obtain the possible data distribution

Algorithm 1 - $evalACCES(FM, L)$

Require: Fingerprint Map $FM = \{(\mathbf{r}_i, \mathbf{m}_i), i = 1, ..., N\}$, locations of interest $L = \{\mathbf{r}_j, j = 1, ..., M\}$.

1: $acces_j = \emptyset$, $j = 1, ..., M$ ▷ $ACCES$ values to return
2: $predictors = GPR(FM)$ ▷ Predictors for each component of a measurement vector
3: **for all** $\mathbf{r}_j \in L$ **do**
4: $acces_j \leftarrow evalCRLB(\mathbf{r}_j, predictors)$
5: **end for**
6: **return** $acces$

over the indoor area along with a confidence in it, which capture the uncertainty of the collected measurements, spatial sparsity of the fingerprints and the spatial smoothness of the underlying true data. This approach is similar to the interpolation proposed in [26] and [24]. With the second step, a bound on the smallest possibly achievable localization error is calculated, given the knowledge and confidence about the collected and interpolated measurements. We assume this bound qualitatively corresponds to the real localization error similarly to [23], where it is used for AP placement optimization in order to improve localization. Algorithm 1 presents an outline of ACCES calculation at a set of locations given a *FM*.

B. Generic Interpolation with Gaussian Processes

Due to the inevitable influence of noise to measuring systems and the difference in sensors across devices, fingerprints should not be considered as deterministic, but rather as probabilistic entities. Thus, fingerprint values should be defined with a *probability distribution* in the form of a *likelihood function*, which shows how probable is to measure a particular value at a location. The likelihood function is usually constructed by considering the measured fingerprint values $\mathbf{m}_i$ (along with the noise) and *interpolating* them to any arbitrary location with coordinates $\mathbf{r}$ based on the distances $\|\mathbf{r} - \mathbf{r}_i\|$. In our approach we use the *predictive distribution* of a GPR estimator to define the likelihood function.

Algorithm Description: One can think of a fingerprint as a sample from a noisy function f of some physical quantity (e.g., WiFi electromagnetic signal, magnetic field of the Earth), where noise is assumed to be Gaussian. In order to estimate the underlying function, one can apply a *regression* technique to the measurement data, so as to obtain a *predictor* that can be used to estimate unknown values at arbitrary locations. Remarkably, with GPR, such a predictor also provides, along with the predicted value, an uncertainty estimate per se as the Gaussian distribution's variance. This uncertainty estimate captures: (i) the spatial sparsity of the measurements (i.e., the more sparse measurements are, the larger is the uncertainty); (ii) the variability of the measurements (i.e., less complex functions are predicted more accurately); and (iii) the noise in measurements (i.e., larger noise leads to worse accuracy).

Given a map of scalar fingerprints FM, i.e., a map where measurements consist of single values, such as magnetic field magnitude, the output of the GPR algorithm is given by:

$$GPRScalar(FM) \rightarrow f(\mathbf{r}) \sim \mathcal{N}(\mu(\mathbf{r}), \sigma^2(\mathbf{r})), \qquad (4)$$

where $\mathcal{N}$ denotes a Gaussian random variable, and $\mu(\mathbf{r})$, $\sigma(\mathbf{r})^2$ denote its mean and variance, respectively. The likelihood function value at $\mathbf{r}$ is given by the *probability density* of the GPR's predictive distribution, which is Gaussian. Fig. 4 depicts the output of GPR applied on noisy scalar sinusoidal data with the uncertainty shown as the standard deviation values.

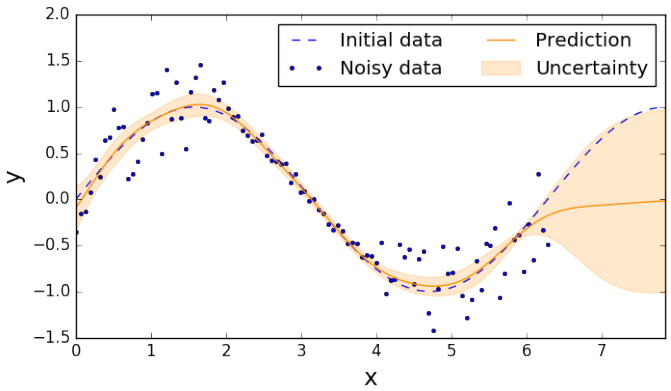

Fig. 4: *GPR*: sin function, noisy samples with smaller noise for $2 \leq x \leq 4$ and no data for $x \geq 6$, GPR prediction and its uncertainty. In the interval of smaller noise, uncertainty decreases, whereas in the region of data unavailability it increases dramatically.

Algorithm 2 - $GPR(FM)$

Require: Fingerprint Map $FM = \{(\mathbf{r}_i, \mathbf{m}_i), i = 1, ..., N\}$.

1: $predictors_k = \emptyset$, $k = 1, ..., d_m$ ▷ Predictors for each component of a measurement vector
2: **for** $k = 1...d_m$ **do**
3: $FM_i^k = \emptyset$, $i = 1, ..., N$ ▷ A sub-map of FM, containing k^{th} component of each fingerprint
4: **for all** $(\mathbf{r}_i, \mathbf{m}_i) \in FM$ **do**
5: $FM_i^k \leftarrow (\mathbf{r}_i, \mathbf{m}_i^k)$ ▷ Constructing the sub-map
6: **end for**
7: $predictor = GPRScalar(FM^k)$ ▷ Obtaining a scalar GPR predictor from the sub-map
8: $predictors_k \leftarrow predictor$
9: **end for**
10: **return** predictors

Multidimensional data: As GPR cannot be directly applied to multidimensional (or vector) data (i.e., $d_m \geq 2$), but only to scalar data (i.e., $d_m = 1$), we need to assume that measurement channels are independent, i.e., magnetic field components vary independently over an area, or separate Wi-Fi APs do not interfere with each other [27]. Thus, GPR can be applied separately to each component $k = 1, ..., d_m$ of fingerprint measurements to obtain d_m predictors, each allowing to estimate the parameters of a Gaussian distribution for one component of a vector-function $\mathbf{f}(\mathbf{r})$ separately (see Algorithm 2). Combining these parameters into a single vector, one obtains the following GPR output from a map FM of vector fingerprints:

$$GPR(FM) \rightarrow \mathbf{f}(\mathbf{r}) \sim \mathcal{N}\left(\boldsymbol{\mu}(\mathbf{r}), diag(\boldsymbol{\sigma}(\mathbf{r}))^2\right), \qquad (5)$$

where $diag(\mathbf{x})$ denotes a diagonal matrix with a diagonal equal to the vector $\mathbf{x}$ and $\mathcal{N}$ denotes a Gaussian random vector. The likelihood function value at $\mathbf{r}$ is the respective probability density function of the *multivariate* Gaussian distribution.

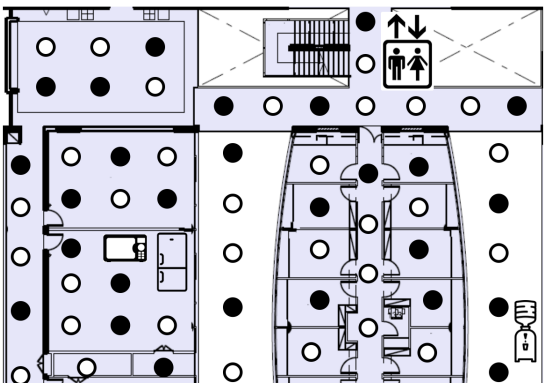

Fig. 5: Black circles denote locations of the collected magnetic fingerprints, white circles denote locations, where measurements are not collected, but predicted using GPR.

Example: Figure 5 demonstrates an indoor environment with the ambient magnetic field of the Earth serving as the source of fingerprint data. Black circles represent locations which constitute a FM collected during offline phase. White circles represent locations, where magnetometer measurements were not collected, but are predicted using GPR in order to obtain a picture of how the magnetic field could be distributed over the whole indoor area.

Choosing parameters: Although GPR is a non-parametric technique and can be used as a black box, some parameters, dependent on the origin of the fingerprints and localization scenarios, must be selected in order to obtain sensible error estimate values.

First, we should choose a *Kernel Function* or a *kernel*, which, in the case of GPR, denotes how spatially near measurements are *correlated* or, in other words, influenced by each other. We opt for the popular *Radial Basis Function* (RBF) kernel, which has the following form:

$$K^{RBF}(\mathbf{r}_i, \mathbf{r}_j) = \exp\left(-\frac{\|\mathbf{r}_i - \mathbf{r}_j\|^2}{2\ell^2}\right), \mathbf{r}_i, \mathbf{r}_j \in \mathbb{R}^{d_r}, \quad (6)$$

where ℓ is a scaling factor. RBF kernels are good to model arbitrary non-periodic and smooth functions, which is the case for physically-driven data, e.g., magnetic and electromagnetic.

Secondly, we should consider the uncertainty due to noisiness and limited sensor accuracy, which can be directly incorporated in the kernel as follows:

$$K(\mathbf{r}_i, \mathbf{r}_j) = K^{RBF}(\mathbf{r}_i, \mathbf{r}_j) + \sigma_k^2 \delta_{ijk}, \quad (7)$$

where σ_k^2 is a noise level for measurement k, and δ_{ijk} is a multi-index Kronecker delta.

Last, the values of ℓ and σ_k must be chosen; ℓ may be picked as the smallest achievable motion magnitude in the particular localization setting, which could be the smallest wheeled robot movement, or human's foot size; the noise level σ_k can be expressed as the sensitivity of the sensors, which is 150 to 600 nT for typical smartphone magnetometer and 0.5-1.0 db for RSSI readings. However, such sensitivity may underestimate the true noise level and, thus, it is preferable to obtain the noise level from empirical data, e.g., collect multiple measurements for each location $\mathbf{r}$ and calculate the standard deviation. Besides, it is not necessary to infer parameter values directly; they can rather be derived using a *parameter estimation* technique to get the best approximation of the data with GPR. Thus, one may consider choosing ℓ and σ_k manually when the fingerprint map is sparse and some prior information is available, or automatically using parameter estimation algorithms when the map is dense.

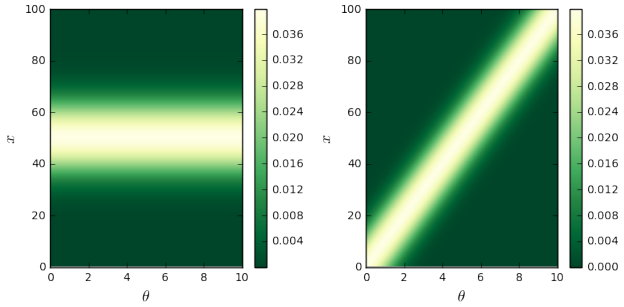

Fig. 6: Likelihood function $p(x|\theta)$ in Gaussian case with variance independent of θ and equal to 100; (a) mean independent of θ and equal to 50; (b) mean changing linearly with θ.

Algorithm 3 - $evalCRLB(\mathbf{r}, predictors)$

Require: Location $\mathbf{r}$, fingerprint $predictors$ such that $\mathbf{m}^k, \boldsymbol{\sigma}^k = predictor_k.predict(\mathbf{r})$ for each $predictor_k \in predictors$, where $\mathbf{m}^k, \boldsymbol{\sigma}^k$ denote $k-$th component of the predicted measurement and its uncertainty, respectively.

1: $\mathcal{I} = evalFIM(\mathbf{r}, predictors)$ ▷ Calculate Fisher Information Matrix as in eq. 12

2: $crlb = sqrt(tr(inv(\mathcal{I})))$

3: **return** $crlb$

Reducing complexity: A drawback of GPR is its computational complexity. Regression takes $\mathcal{O}(N^3)$ operations, where N is the number of data samples. Therefore, the GPR calculation may be very costly for large fingerprint maps though being one-time procedure unless FM is changed. To overcome this limitation, we propose to split the indoor area I into parts, with each part containing a moderate amount of measurements, i.e., split each building into floors, floors into rooms, corridors, etc. and calculate GPR only locally. This seems to be a natural solution, since distant fingerprints are not interrelated.

C. Cramer-Rao Lower Bound

Given the interpolated fingerprint values obtained by GPR, we can derive the CRLB on the best possibly achievable accuracy of any unbiased location estimator, i.e., localization algorithm. We emphasize that our interest is neither in the CRLB's absolute value, nor in the possibility of some biased estimators outperforming this bound; we are rather curious about the CRLB's behavior. Algorithm 3 provides an outline of the CRLB calculation.

Algorithm Description: The CRLB computation requires the intermediate calculation (line 1 of Algorithm 3) of a *Fisher Information Matrix* (FIM), which shows how much information an observable random variable (or vector) carries about

some deterministic parameter it depends on, e.g., how much sensor measurements at an unknown location could shed a light on its coordinates. Fig. 6 shows an example, where different likelihood functions depict the probability of measuring x for different values of a scalar parameter θ, with color coding the probability value. On the left side, the likelihood does not depend on the parameter value and, thus, x does not carry any information about θ, whereas on the right side, the likelihood is unique for each parameter value, thus, by observing x, one can eventually infer the value of θ.

Now, we discuss an analytical representation of the FIM, inferred from the GPR interpolation, with the derivations available in appendix section. Let $\boldsymbol{\theta} \in \mathbb{R}^{d_\theta}$ denote a vector-parameter that is being estimated and $\mathbf{x} \in \mathbb{R}^{d_x}$ denote a random vector, the distribution of which is dependent on $\boldsymbol{\theta}$. Then, the FIM is

$$\mathcal{I}(\boldsymbol{\theta}) = [\mathcal{I}(\boldsymbol{\theta})_{ij}]_{i,j=1}^{d_\theta,d_\theta} = -\mathbb{E}\left(\frac{\partial^2 \log p(\mathbf{x}|\boldsymbol{\theta})}{\partial \boldsymbol{\theta}_i \partial \boldsymbol{\theta}_j}\right), \quad (8)$$

where $\boldsymbol{\theta}_i$ denotes the $i-$th component of $\boldsymbol{\theta}$, $\mathcal{I}(\boldsymbol{\theta})_{ij}$ denotes an element of the matrix $\mathcal{I}(\boldsymbol{\theta})$ in the $i-$th row and the $j-$th column, $p(\mathbf{x}|\boldsymbol{\theta})$ is a likelihood showing the probability of sampling $\mathbf{x}$ from its distribution given the parameters $\boldsymbol{\theta}$, and mathematical expectation $\mathbb{E}$ is taken over $\mathbf{x}$. In the case of GPR, the likelihood is given by probability density function of a Gaussian distribution.

The CRLB is given by the following bound on the RMSE of the estimation:

$$RMSE \geq \sqrt{tr(\mathcal{I}^{-1}(\boldsymbol{\theta}))} = ACCES, \quad (9)$$

where we let *ACCESS* to be such bound.

Example: Figure 7 demonstrates CRLB values calculated for a set of locations (of both collected and predicted measurements) inside an indoor environment during the offline phase. Lower CRLB (dark green circles) values imply better accuracy during the online phase, whereas higher values (light yellow circles) imply lower accuracy: (i) In the room with the microwave and fridge additional magnetic perturbations occur, and accuracy is expected to be higher than in another areas; (ii) Also, in other parts of the building close to the escalator, elevator and water dispenser, where magnetic disturbances occur, accuracy is expected to be relatively good; and (iii) Far from magnetic disturbance, like in the top left part of the building, accuracy is expected to be worse, which also applies to locations across the corridors where magnetic field does not vary significantly.

Numerical Calculation: As it is shown in eq. 12 of appendix section, computation of the FIM involves evaluation of a *Hessian* matrix, which raises a concern of its computation. One approach is to derive it analytically from the expression for the predictive distribution of GPR. The main drawback of this approach is that the analytical form depends on the particular choice of kernel and is therefore not generalizable. Another approach is a numerical approximation based on finite difference schemes. With this approach, it is possible to evaluate a Hessian matrix for any values of $\boldsymbol{\theta}$ with sufficient precision. We stick to the latter approach, and for the numerical calculation we utilize the *Numdifftools* package for the *Python*, assuming the conditions for differentiability are satisfied. Last, we let $\boldsymbol{\theta} \triangleq \mathbf{r}$ and $\mathbf{x} \triangleq \mathbf{m}$ and, thus, obtain the desired CRLB for fingerprint-based localization accuracy estimation.

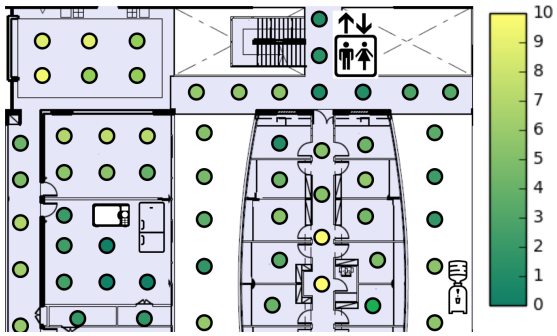

Fig. 7: CRLB values calculated at a set of locations inside indoor environment with the fingerprint data comprising magnetometer readings.

V. Experimental Evaluation

This section presents an experimental evaluation of the proposed accuracy estimation framework. We start out with our experimental methodology and setup followed by our experimental study.

A. Methodology

Real Dataset: We use datasets covering magnetometer readings to show the applicability of our analysis to fingerprint data of any modeling complexity. This dataset, obtained from the UJIIndoorLoc-Mag database [28], consists of 270 continuous training and 11 testing samples with each sample comprising set of discrete samples collected along 8 corridors of a 260 m^2 lab, with a total of 40,159 discrete captures, each containing readings from the magnetometer, the accelerometer and the orientation sensor taken by an Android smartphone.

Training samples are split into two groups: "lines" and "curves". Samples from the first group represent a sequence of measurements taken along a single corridor in two opposing directions with 5 passes for each line, whereas samples from the latter group are taken along each possible pair of connected corridors with 5 passes for each curve. Testing samples represent a sequence of measurements obtained over complex routes consisting of several corridors.

Dataset Construction: We consider this dataset consisting of 1-D data (but our solution can be applied directly to 2-D and 3-D data without any modifications) of fingerprints taken only over corridors (similarly to the approach proposed in [6]); thus, we consider the venue being split into the sub-areas (corridors), which we study separately. For the quality assessment of a *FM*, we are interested only in the 3 values of magnetometer readings, thus, we discard accelerometer and orientation data. To simplify the localization scenarios we use only "lines" group of samples both for the *FM* construction and testing phases. Moreover, we consider only passes in one direction, thus, we leave only 5 sequences of readings for each corridor. The *FM* data used for the interpolation step consists of the 4 combined sequences of fingerprints per corridor with the 5^{th} used for navigability score calculation purposes during the testing step. In particular, for the sake of RMSE calculation, each of five attempt sequences are one by one chosen as testing

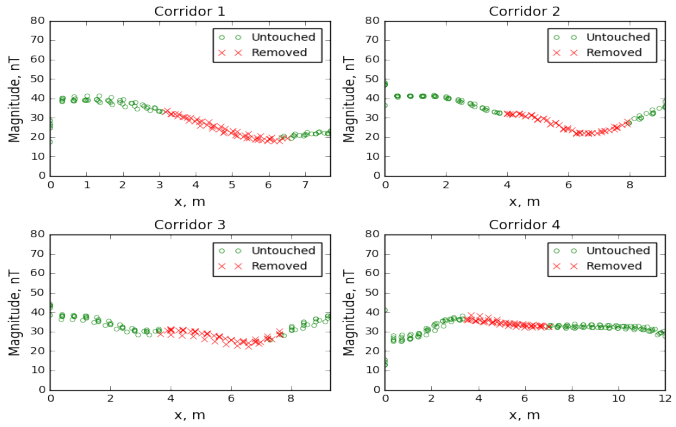

(a) Magnetic field magnitude in "cut" scenario.

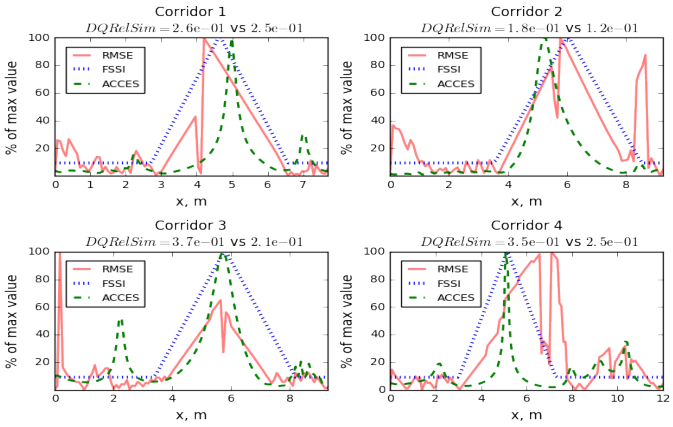

(b) ACCES vs FSSI vs RMSE in "cut" scenario.

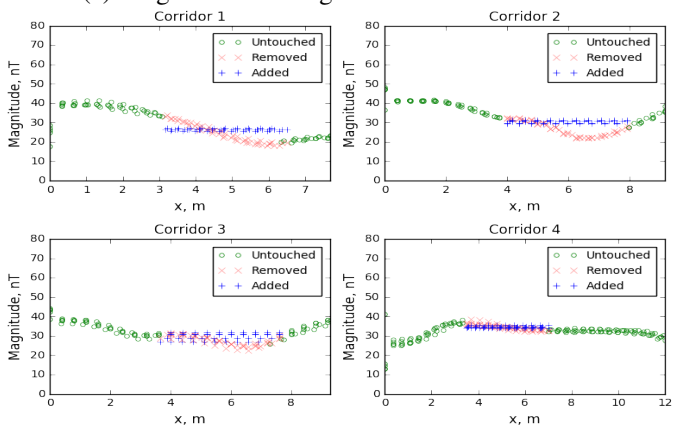

(c) Magnetic field magnitude in "flat" scenario.

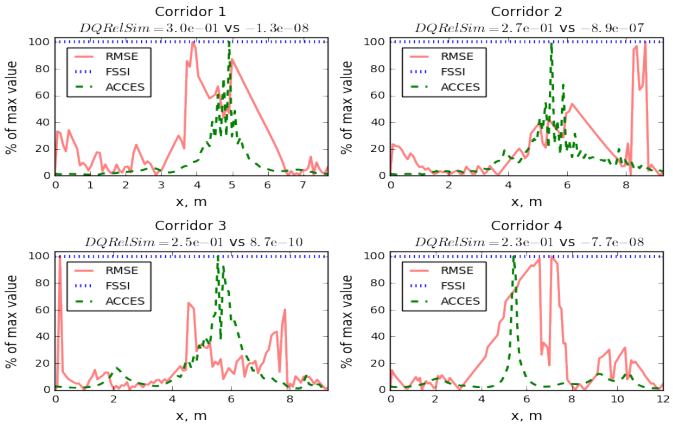

(d) ACCES vs FSSI vs RMSE in "flat" scenario.

Fig. 8: Magnetic field magnitude and ACCES vs FSSI vs RMSE for 4 corridors; $DQRelSim(RMSE, ACCES)$, $DQRelSim(RMSE, FSSI)$ values on top.

data and the rest four as FM data, thus, producing five FMs and five testing sequences.

Algorithms and Metrics: We utilize three algorithms in order to assess our solution: (i) WkNN localization algorithm for evaluation of the real localization RMSE and subsequent comparison against the values of navigability scores; (ii) FSSI, which is the baseline outlined in Section III-C; and (iii) ACCES, which is the framework proposed in this work. The comparison of RMSE against the ACCES and FSSI values is performed via the $DQRelSim$ metric, introduced in Section III. For the given metric, we use a DTW window size equal to 20% of the sequence length, which appeared to be provide a reasonable performance-utility trade-off in our experiments.

For the real indoor localization scenario we utilize WkNN localization algorithm and obtain RMSE using the ground truth location from the dataset. Given the fingerprint map FM and a currently observed fingerprint $\mathbf{m}$, WkNN calculates the Euclidean distance against it and all of the fingerprints, i.e., $d_i = ||\mathbf{m} - \mathbf{m}_i||, \forall(\mathbf{r}_i, \mathbf{m}_i) \in FM$. Then, weights $w_i \propto d_i^{-1}$ are assigned to each fingerprint and the k most significant are chosen. The user's location is calculated using a convex combination of those k fingerprints' locations. In our experiments we set $k = 3$.

FSSI is the naïve approach that allows to capture the spatial sparsity of fingerprints and is evaluated as in equation 3. Larger FSSI values correspond to smaller numbers of fingerprints per area, thus, potentially, worse accuracy.

ACCES is the navigability score proposed in this paper. GPR-based interpolation is done via the open-source *scikit-learn* library for Python with kernel parameters optimized using the in-built *Broyden–Fletcher–Goldfarb–Shanno* algorithm.

Outline of the Experiments: To evaluate the qualitative behavior of ACCES, we performed 3 experiments: comparison of the ACCES and FSSI against the RMSE values based on relative similarity in: (i) "cut" scenario, where a continuous sequence of measurements is removed from *FM*, which corresponds to unavailability of a part of the venue during the FM construction; (ii) "flat" scenario, where a continuous sequence of measurements from *FM* is made constant, which corresponds to insufficient magnetic field variation in the corridor of the building without steel elements in its construction; and (iii) "sparse" scenario, where fingerprints are removed from *FM* uniformly, which relates to variability of a sensor reading rate during fingerprint collection.

B. Performance Evaluation

To assess the qualitative behavior of ACCES and naïve FSSI approach, we evaluate them over test locations along

TABLE II: Similarity of RMSE values with FSSI and ACCES for "cut", "flat" and "sparse" scenarios over 8 test corridors. For "sparse" scenario the results for 75% fingerprints removed are provided.

	$DQRelSim(RMSE, *)$					
	"Cut"		"Flat"		"Sparse"	
Corridor	ACCES	FSSI	ACCES	FSSI	ACCES	FSSI
1	3.7e-01	2.1e-01	3.0e-01	-1.3e-08	2.5e-01	-1.6e-07
2	3.5e-01	2.5e-01	2.7e-01	-8.9e-07	2.7e-01	-6.7e-08
3	3.5e-01	2.3e-01	2.5e-01	8.7e-10	3.5e-01	2.9e-08
4	2.6e-01	2.5e-01	2.3e-01	-7.7e-08	2.7e-01	7.8e-08
5	1.8e-01	1.2e-01	1.5e-01	2.1e-06	6.4e-02	-1.8e-07
6	2.0e-01	3.0e-01	1.4e-01	-3.4e-08	1.8e-01	-3.5e-08
7	2.3e-01	2.2e-01	1.1e-01	-7.3e-10	1.5e-01	1.7e-08
8	3.3e-01	1.9e-01	1.1e-01	-7.3e-08	3.5e-01	-9.2e-09

the 8 corridors in "cut", "flat" and "sparse" scenario, and compare them against the respective RMSE values using the $DQRelSim$ metric. Table II provides the $DQRelSim$ values in all 8 corridors, whereas on the graphs we present the results for only 4 of them in order to preserve space.

Fig. 8(a) shows the distribution of the magnetic field magnitude for the complete and "cut" *FM* data, when a sufficiently large interval of fingerprints is removed. Fig. 8(b) shows the respective distributions of the real localization error RMSE and navigability scores FSSI and ACCES (normalized to the maximum value). Both FSSI and ACCES show reasonable behavior patterns and yield good similarity values $DQRelSim$ to RMSE in the range of $0.1 - 0.4$.

Fig. 8(c) shows the distribution over the corridor of the magnetic field magnitude for the initial and "flat" *FM* data, when a sufficiently large interval of the measurements is made constant. Fig. 8(d) shows the respective distributions of the real localization error RMSE and the navigability scores FSSI and ACCES. Remarkably, ACCES shows a correspondence to the RMSE, especially in the interval of measurements' stagnation and yields $DQRelSim$ values greater than 0.2, which indicates good similarity; on the other hand, FSSI does not detect any potentially problematic areas, keeping a nearly constant value level over the corridors and yielding nearly zero $DQRelSim$ values, which indicates no similarity.

Fig. 9 shows the ACCES values (left column) and RMSE values (right column) for 3 cases: (i) complete *FM*; (ii) half of fingerprints removed uniformly from the *FM*; and (iii) 75% of fingerprints removed uniformly from the *FM*. Overall, we note that both ACCES and RMSE values indeed grow as the number of the fingerprints decreases, because collecting fewer data leads to accuracy degradation.

Conclusions and Future Directions

This paper introduced a novel framework for offline accuracy estimation in fingerprint-based localization services. The proposed ACCES method operates in two phases: the *interpolation* phase, in which an arbitrary fingerprint map is used as input for *Gaussian Process Regression*, yielding the fingerprint prediction at any location in the form of a *likelihood* function; and the *accuracy estimation* phase, in which the likelihood function is used for the calculation of *Cramer-Rao Lower Bound* on localization error, which is considered as a

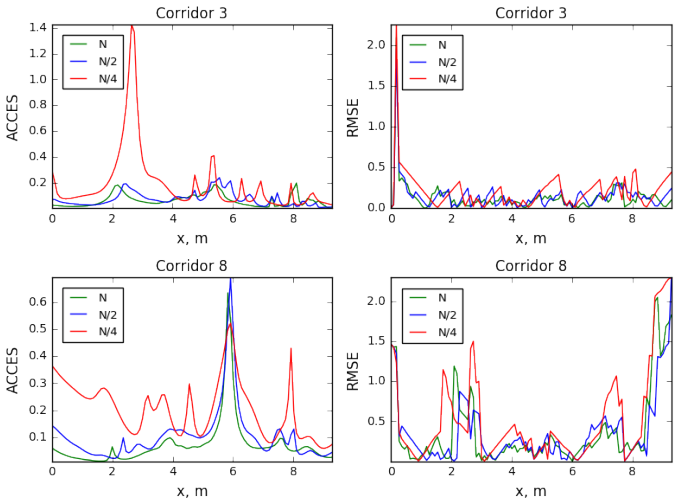

Fig. 9: ACCES and RMSE values for 2 corridors in "sparse" scenario.

navigability score, qualitatively describing the real localization performance. We evaluated our framework using a prototype developed in Python and open-source libraries for GPR and numerical calculations. Our experimental study reveals that the obtained navigability score corresponds well to the real localization accuracy error.

In the future, we aim to apply our framework on Wi-Fi and magnetic fingerprints together over a 2-D area, as opposed to the 1-D case studied in this paper. We also plan to compare out approach with other offline and online accuracy estimation algorithms and also complete integration issues with the Anyplace open-source indoor navigation service.

Acknowledgments

We would like to thank the Anyplace community for their continuous support. The last author's research is supported by the Alexander von Humboldt-Foundation, Germany.

References

[1] H. Wang, S. Sen, A. Elgohary, M. Farid, M. Youssef, and R. R. Choudhury, "No need to war-drive: unsupervised indoor localization," in *Proceedings of the 10th international conference on Mobile systems, applications, and services*. ACM, 2012, pp. 197–210.

[2] D. Zeinalipour-Yazti, C. Laoudias, K. Georgiou, and G. Chatzimilioudis, "Internet-based indoor navigation services," *IEEE Internet Computing*, 2017 (in-press).

[3] D. Lymberopoulos, J. Liu, X. Yang, R. R. Choudhury, . ., C. Laoudias, D. Zeinalipour-Yazti, Y.-K. Tsai, and e. al., "A realistic evaluation and comparison of indoor location technologies: Experiences and lessons learned," in *Proceedings of the 14th IEEE/ACM International Symposium on Information Processing in Sensor Networks*, 2015.

[4] C. E. Rasmussen, "Gaussian processes for machine learning," *The MIT Press*, 2006.

[5] A. Konstantinidis, G. Chatzimilioudis, D. Zeinalipour-Yazti, P. Mpeis, N. Pelekis, and Y. Theodoridis, "Privacy-preserving indoor localization on smartphones," *IEEE Transactions on Knowledge and Data Engineering*, vol. 27, no. 11, pp. 3042–3055, Nov 2015.

[6] D. Ahmetovic, C. Gleason, K. Kitani, H. Takagi, and C. Asakawa, "Navcog: turn-by-turn smartphone navigation assistant for people with visual impairments or blindness," in *Web for All Conference*. ACM, 2016.

[7] A. Baniukevic, C. S. Jensen, and H. Lu, "Hybrid indoor positioning with wi-fi and bluetooth: Architecture and performance," in *Proceedings of the 14th IEEE International Conference on Mobile Data Management*, 2013, pp. 207–216.

[8] M. Youssef and A. Agrawala, "The horus wlan location determination system," in *Proceedings of the 3rd international conference on Mobile systems, applications, and services*. ACM, 2005, pp. 205–218.

[9] J. Biswas and M. M. Veloso, "Wifi localization and navigation for autonomous indoor mobile robots," *IEEE International Conference on Robotics and Automation*, 2010.

[10] K. Georgiou, T. Constambeys, C. Laoudias, L. Petrou, G. Chatzimilioudis, and D. Zeinalipour-Yazti, "Anyplace: A crowdsourced indoor information service," in *2015 16th IEEE International Conference on Mobile Data Management*, vol. 1. IEEE, 2015, pp. 291–294.

[11] J. Haverinen and A. Kemppainen, "Global indoor self-localization based on the ambient magnetic field," *Robotics and Autonomous Systems*, vol. 57, no. 10, pp. 1028–1035, 2009.

[12] J. Blankenbach and A. Norrdine, "Position estimation using artificial generated magnetic fields," in *Indoor Positioning and Indoor Navigation (IPIN), 2010 International Conference on*. IEEE, 2010, pp. 1–5.

[13] C. E. Galván-Tejada, J. P. García-Vázquez, J. I. Galván-Tejada, J. R. Delgado-Contreras, and R. F. Brena, "Infrastructure-less indoor localization using the microphone, magnetometer and light sensor of a smartphone," *Sensors*, vol. 15, no. 8, pp. 20 355–20 372, 2015.

[14] R. Harle, "A survey of indoor inertial positioning systems for pedestrians." *IEEE Communications Surveys and Tutorials*, vol. 15, no. 3, pp. 1281–1293, 2013.

[15] H. Liu, H. Darabi, P. Banerjee, and J. Liu, "Survey of wireless indoor positioning techniques and systems," *IEEE Transactions on Systems, Man, and Cybernetics, Part C: Applications and Reviews*, vol. 37, no. 6, pp. 1067–1080, 2007.

[16] F. Gustafsson and F. Gunnarsson, "Mobile positioning using wireless networks: possibilities and fundamental limitations based on available wireless network measurements," *IEEE Signal processing magazine*, vol. 22, no. 4, pp. 41–53, 2005.

[17] S. Jung, C.-o. Lee, and D. Han, "Wi-fi fingerprint-based approaches following log-distance path loss model for indoor positioning," in *Intelligent Radio for Future Personal Terminals (IMWS-IRFPT), 2011 IEEE MTT-S International Microwave Workshop Series on*. IEEE, 2011, pp. 1–2.

[18] L. Petrou, G. Larkou, C. Laoudias, D. Zeinalipour-Yazti, and C. G. Panayiotou, "Crowdsourced indoor localization and navigation with anyplace," in *Proceedings of the 13th international conference on Information Processing in Sensor Networks*, 2014, pp. 331–332.

[19] B. Li, J. Salter, A. G. Dempster, and C. Rizos, "Indoor positioning techniques based on wireless lan," in *1st Intl. Conf. on Wireless Broadband and Ultra Wideband Communications*, 2006, pp. 13–16.

[20] R. Elbakly and M. Youssef, "Cone: Zero-calibration accurate confidence estimation for indoor localization systems," *arXiv preprint arXiv:1610.02274*, 2016.

[21] H. Lemelson, M. B. Kjærgaard, R. Hansen, and T. King, "Error estimation for indoor 802.11 location fingerprinting," in *International Symposium on Location-and Context-Awareness*. Springer, 2009, pp. 138–155.

[22] A. M. Hossain and W.-S. Soh, "Cramer-rao bound analysis of localization using signal strength difference as location fingerprint," in *INFOCOM, 2010 Proceedings IEEE*. IEEE, 2010, pp. 1–9.

[23] M. Stella, M. Russo, and D. Begusic, "Rf localization in indoor environment," *Radioengineering*, vol. 21, no. 2, pp. 557–567, 2012.

[24] S. Kumar, R. M. Hegde, and N. Trigoni, "Gaussian process regression for fingerprinting based localization," *Ad Hoc Networks*, vol. 51, pp. 1–10, 2016.

[25] N. Swangmuang and P. Krishnamurthy, "Location fingerprint analyses toward efficient indoor positioning," in *Pervasive Computing and Communications, 2008. PerCom 2008. Sixth Annual IEEE International Conference on*. IEEE, 2008, pp. 100–109.

[26] N. Akai and K. Ozaki, "Gaussian processes for magnetic map-based localization in large-scale indoor environments," in *Intelligent Robots and Systems (IROS), 2015 IEEE/RSJ International Conference on*. IEEE, 2015, pp. 4459–4464.

[27] K. Kaemarungsi and P. Krishnamurthy, "Properties of indoor received signal strength for wlan location fingerprinting," in *Mobile and Ubiquitous Systems: Networking and Services, 2004. MOBIQUITOUS 2004. The First Annual Intl. Conf. on*. IEEE, 2004, pp. 14–23.

[28] J. Torres-Sospedra, D. Rambla, R. Montoliu, O. Belmonte, and J. Huerta, "Ujiindoorloc-mag: A new database for magnetic field-based localization problems," in *Indoor Positioning and Indoor Navigation (IPIN), 2015 International Conference on*. IEEE, 2015, pp. 1–10.

VI. Appendix

In this section we derive CRLB for the predictive distribution of the GPR. As we discussed, in the case of GPR, the predictive distribution, i.e., the distribution of noisy function values for some parameter value, is Gaussian

$$\mathbf{x}|\boldsymbol{\theta} \sim \mathcal{N}(\boldsymbol{\mu}(\boldsymbol{\theta}), \Sigma(\boldsymbol{\theta})),$$

where $\mathbf{x}$ is the predicted value for the parameter value $\boldsymbol{\theta}$, $\boldsymbol{\mu}(\boldsymbol{\theta})$ and $\Sigma(\boldsymbol{\theta})$ are the mean vector and the covariance matrix, respectively. We assume that the covariance matrix is diagonal. Thus, the log-likelihood function for the predicted value $\mathbf{x}$ given the parameter $\boldsymbol{\theta}$ is:

$$\begin{aligned}\log p(\mathbf{x}|\boldsymbol{\theta}) \sim -\frac{1}{2}(\mathbf{x}-\boldsymbol{\mu}(\boldsymbol{\theta}))^T\Sigma^{-1}(\boldsymbol{\theta})(\mathbf{x}-\boldsymbol{\mu}(\boldsymbol{\theta}))- \\ -\frac{1}{2}\log|\Sigma(\boldsymbol{\theta})|,\end{aligned} \tag{10}$$

where $|\cdot|$ denotes a *determinant* of a square matrix. Plugging (10) into (8) results in the following expression for the FIM:

$$\begin{aligned}\mathcal{I}(\boldsymbol{\theta}) = \frac{1}{2}\cdot\mathbb{E}\Bigg[\frac{\partial^2}{\partial\boldsymbol{\theta}_i\partial\boldsymbol{\theta}_j}\big[(\mathbf{x}-\boldsymbol{\mu}(\boldsymbol{\theta}))^T\Sigma^{-1}(\boldsymbol{\theta})(\mathbf{x}-\boldsymbol{\mu}(\boldsymbol{\theta}))+ \\ +\log|\Sigma(\boldsymbol{\theta})|\big]\Bigg].\end{aligned} \tag{11}$$

Subsequently, it can be transformed to

$$\begin{aligned}\mathcal{I}(\boldsymbol{\theta}) = \frac{1}{2}\sum_{k=1}^{d_x}\Big[(\sigma_k^2+\mu_k^2)H(\sigma_k^{-2}) + H(\mu_k^2\sigma_k^{-2})- \\ -2\mu_k H(\mu_k\sigma_k^{-2}) + 2H(\log\sigma_k)\Big],\end{aligned} \tag{12}$$

where we omit the arguments of the mean and variance for the sake of readability, $H(\cdot)$ is a *Hessian Matrix*, μ_k is the $k-$th component of μ and σ_k is the $k-$th diagonal element of Σ. The CRLB is then given by the inequality:

$$cov(\hat{\boldsymbol{\theta}}) \geq \mathcal{I}^{-1}(\boldsymbol{\theta}),$$

where $\hat{\boldsymbol{\theta}}$ is any unbiased estimator of $\boldsymbol{\theta}$, and $cov(\cdot)$ its covariance matrix. Now the Root Mean Square Error of the estimate is given by the square root of the *trace* of the covariance matrix, thus:

$$RMSE \geq \sqrt{tr(\mathcal{I}^{-1}(\boldsymbol{\theta}))}. \tag{13}$$

For the case of the scalar parameter θ, i.e., $d_\theta = 1$ (which is considered in our experimental evaluation), the FIM is a one-element matrix, and, thus, the derived formulas are directly applicable with a Hessian matrix being just a second-order partial derivative.